This draft is published as: First-principles molecular dynamics modeling of the LiCl-KCl molten salt system, Amelia Bengtson, Hyo On Nam, Saumitra Saha, Ridwan Sakidja, Dane Morgan, Computational Materials Science, Volume 83, Pages 362–370, 2014

First-principles molecular dynamics modeling of the LiCl-KCl molten salt system

Amelia Bengtson, Hyo On Nam, Saumitra Saha, Ridwan Sakidja, Dane Morgan*

Department of Materials Science and Engineering, University of Wisconsin-Madison, Madison, Wisconsin 53706, USA

ABSTRACT

Properties of molten salts are of interest for a wide-range of applications, including nuclear waste partitioning, heat transfer fluids, and synthesis methods. While there has been extensive work showing the value of molecular modeling with interatomic potentials to predict molten salt properties there have been very limited studies of molten salts from a fully first-principles approach. In order to establish optimal approaches and their strengths and limitations in first-principles molten salt modeling, this work provides extensive first-principles molecular dynamics simulations of the LiCl-KCl molten salt system that are validated against existing literature. The basic thermokinetic properties of volume, thermal expansion, bulk modulus, and diffusivity, are calculated for LiCl, KCl and the eutectic LiCl-KCl liquids at multiple temperatures. Convergence testing reveals 216-atom unit cells and simulation times of 6-12 ps are sufficient to provide results with acceptable uncertainties and agreement with experimental data. The results provide a framework of first principles molecular dynamics simulations in the LiCl-KCl molten salt system that can be extended in future research to predict less well-established properties, e.g., the behavior of solutes.

Keywords: First-principles, molecular dynamics, LiCl-KCl, molten salt, modeling

*Corresponding author
Dane Morgan
Associate Professor,
Department of Materials Science and Engineering,
University of Wisconsin-Madison, Madison, Wisconsin 53706
Email: ddmorgan@wisc.edu

This draft is published as: First-principles molecular dynamics modeling of the LiCl-KCl molten salt system, Amelia Bengtson, Hyo On Nam, Saumitra Saha, Ridwan Sakidja, Dane Morgan, Computational Materials Science, Volume 83, Pages 362–370, 2014

1. Introduction

The aim of this paper is to explore the applicability of first-principles molecular dynamics (FPMD) simulations to the prediction of properties of LiCl-KCl molten salt system with various compositions (mole fraction of LiCl=1, 0.58, and 0). In particular we seek to obtain converged liquids with stable structure factors from FPMD, calculate volumes, coefficients of thermal expansion, bulk moduli, species diffusion, and the Gibbs free energy of mixing as a function of temperature, and determine if error bars (precision) and accuracy are adequate with present simulation tools to guide experiments.

Measurements on molten salts can be limited by costly and demanding experiments and computational simulations provide a low cost alternative to experiments and can rapidly explore many different temperatures and salt compositions. However, FPMD methods have been applied only rarely to direct calculation of salt properties. Detailed calculations, with careful assessment of uncertainties and comparison to experiments, are needed to establish the optimal approaches and their limitations.

We focus the LiCl-KCl as it is a system of considerable interest for the nuclear community with both extensive quality data for validation and yet many open questions that can be investigated with the methods being considered here. Eutectic LiCl-KCl (58% LiCl, 42% KCl), is a common molten salt used in electrorefining of spent nuclear fuel to separate actinides and other fission products [1-4]. While the basic salt properties are known and can be used to validate our approaches, the thermokinetics of solutes within LiCl-KCl are not well characterized and can be a subject of future modeling [1, 2, 5-7].

The primary goal of the present work is to validate the practicality of direct FPMD approaches for molten salt studies, which are an increasingly viable alternative to the more commonly used interatomic potential molecular dynamics (IPMD) simulations.

In classical IPMD simulations, Newton's equations of motion are solved in a system where interactions between atoms are described by an interatomic potential, which typically contains the physics of ionic repulsion, attraction, dispersion and polarization. IPMD can be used to predict many properties of salts and their solutes [8-12] and is computationally many orders of magnitude faster than FPMD. However, each new salt and each solute and charge state requires fitting a different potential, which can be time consuming and is subject to the inevitable uncertainty of fitted potentials. Furthermore, such potentials do not typically treat the electronic structure explicitly, and therefore cannot easily be used to track electronic properties (e.g., magnetic moments) or redox reactions that might occur between species (although relative stabilities of equivalent impurities have been studied [13]).

FPMD simulations are similar to IPMD in that Newton's equations of motion are also solved, but the atomic interactions are calculated directly from first-principles in FPMD calculations. FPMD therefore requires no fitting to experimental or computed data and provides access to the full electronic structure of the material at every step. The main disadvantage is that FPMD calculations are very computationally intensive and therefore limited to much smaller systems and shorter simulation times than IPMD.

FPMD simulations have successfully modeled liquids such as $CaAl_2O_4$ [14], $CaMgSi_2O_6$ [15], $MgSiO_3$ [16], Ni alloys [17] and ionic liquids [18]. The NaCl and KCl molten salt systems were studied with density-functional-based tight-binding methods (DFT-TB) [19]. While DFT-TB methods are similar to FPMD, they are not fully self-consistent. Furthermore, volumes within the work of Hazebroucq, et al. [19] were fixed to experimental values rather than predicted. FPMD simulations were conducted in the liquid Flibe (Li_2BeF_4) using the Car–Parrinello method [20], but the focus was primarily on diffusion, again at a fixed experimental volume. These limited studies to date show that these methods can be used effectively, but do not provide an extensive enough study of basic properties to establish optimal approach or assess limitations (e.g., in the ability to predict volumes).

Our study is the first full FPMD study on molten salt systems with fully relaxed volumes. Specifically, we will study the LiCl-KCl system and extend previous FPMD work on molten salt systems [20] to include calculations of equilibrium volume, convergence testing on key parameters as a function of unit cell size and simulation time, statistical errors on all values, and rigorous comparison to experiments, when possible. The LiCl-KCl molten salt system has been studied extensively with classical interatomic potential molecular dynamics [8-12] and this data was used for comparison.

2. Computational methods

A combination of first-principles molecular dynamics (FPMD) and interatomic potential molecular dynamics (IPMD) was used in this research. All liquids were equilibrated with IPMD and the final converged structure was used to start the FPMD calculation. FPMD calculations starting from the IPMD liquid reach equilibration within 0.3 ps. The technique of starting FPMD calculations from the liquid created with IPMD has been used successfully in the literature [17, 21]. Note that it might seem to defeat at least part of the purpose of using FPMD if a potential needs to be developed for IPMD to initiate the FPMD calculations. However, while we do not demonstrate it here, it is reasonable to expect the FPMD is quite insensitive to the quality of the IPMD initiation, provided it gets qualitative structural features approximately correct. Thus we expect that no significant time will have to be spent on potential development for IPMD simulations provided they are used for no more than initiating a FPMD simulation.

For the pure LiCl and KCl, we started simulations with crystalline LiCl and KCl structure. In case of the LiCl-KCl eutectic mixture (58% LiCl, 42% KCl), initial configuration of atoms was created from Packmol [22], a code designed to randomly pack atoms into a given volume. While IPMD was typically initiated with a crystalline structure for LiCl and KCl, a randomly distributed initialization of the LiCl system from Packmol (see Computational methods section) also shows a converged liquid structure after the IPMD equilibration and showed same radial distribution functions as initialization from a crystal structure. All IMPD simulations were run with the LAMMPS [23] using the Born-Mayer-Huggins potentials for LiCl and KCl [9] with a radial cutoff of approximately half the lattice parameter for a given unit cell (6, 7, 9, 11, 15 Å for 64, 100, 216, 400, and 1000 atom unit-cells). Formal charges were used for Li (+1), Cl (-1), and K (+1). Simulations, unless otherwise noted, contained 216 atoms. The timestep was 0.001 ps and thermal data was outputted every 100 steps.

A series of ensembles was used to equilibrate the liquid structures. The NVE ensemble with velocities generated from random numbers was run for 5,000 steps to bring the system to the correct temperature. Next, a crude Berendsen barostat [24] for 50,000 steps brought the system to the target pressure. Then, simulations with the NPT ensemble (using the Nosé-Hoover thermostat and barostat) were run for 50,000 time steps for pure LiCl and KCl (500,000 for LiCl-KCl) to equilibrate system at desired pressure and temperature. The lattice was averaged over last quarter of the NPT time steps and used to start the NVT simulation. The NVT ensemble was run for 100,000 time steps for LiCl and KCl (600,000 for LiCl-KCl) for a final equilibration. The resulting structure file was resized for multiple volumes around the experimental volume. Each volume was run with the NVT ensemble for an additional 100,000 time steps. The resulting structure and velocities were used to initialize the VASP NVT simulations.

All FPMD simulations were run with the *Vienna Ab-Initio Simulation Package* VASP version 5.2.11 [21, 25, 26]. PAW-PBE potentials supplied with the VASP package were used for Li (s1p0 17Jan2003), Cl (s2p5 17Jan2003) and K (p6s1 K_sv 06Sep2000). All simulations were run with the canonical ensemble (NVT) using a Nosé thermostat [27] with a Nosé-mass with a period of 40 time steps. Note that the NPT ensemble is not available for VASP versions earlier than 5.3.2, which was recently released. Energy cutoff of 420 eV and a 1×1×1 k-point mesh were used. Charges were calculated within the VASP code. A time step of 0.002 ps was used, which

gave an energy drift of < 1 meV/atom/ps, a value similar to that seen in other FPMD simulations [17]. Simulations were run for 3,000 time steps (unless noted). Dispersion was added through the semi-empirical DFT-D2 method [28]. The DFT-D method has been shown to work well for ionic liquids [18]. Three compositions are considered within the 64-atom unit cell: LiCl (32 Li atoms, 32 Cl atoms), KCl (32 K atoms, 32 Cl atoms) and LiCl-KCl near the eutectic composition (19 Li atoms, 32 Cl atoms, 13 K atoms; 59.4% LiCl). Within the 216-atom unit cell, the eutectic composition is 63 Li atoms, 108 Cl atoms, and 45 K atoms (58.3% LiCl).

Periodic boundary conditions were used in both IPMD and FPMD and simulations represent an infinite bulk material. The pressure, temperature, volume and energy of the ensemble are the statistical averages over many time steps. The standard deviation in the mean was calculated from the autocovariance function [29]. To calculate the equilibrium volume with the NVT ensemble, calculations were run at multiple fixed volumes. The resulting pressures, volumes and their associated errors were fit with a Murnaghan equation of state [30] to determine the equilibrium volume and bulk modulus.

The pressure at a finite temperature includes both a kinetic energy and virial force term [31]:

$$PV = Nk_BT + \langle W \rangle \quad (1)$$

VASP (versions prior to 5.3.2) does not automatically include the kinetic energy term in the pressure. The kinetic energy term, $\frac{Nk_BT}{V}$, was added in post-processing to the pressure for each simulation. This term is usually on the order of 0.35-0.52 GPa in the temperature range 800-1096 K for the LiCl-KCl system.

Diffusion is related through the slope of the mean squared displacement (MSD) by the Einstein equation [31, 32]:

$$D = \frac{1}{6}\lim_{t\to\infty}\frac{d}{dt}(MSD) \quad (2)$$

In practice, D was determined by fitting a linear function to MSD(t) for a subset of the times, as described below. The MSD is determined by a multiple time origin average [32]:

$$MSD(t) = \langle \Delta r^2(t) \rangle = \frac{1}{N}\frac{1}{n_t}\sum_{j=0}^{n_t}\sum_{i=0}^{N}\left(r_i(t_{0j}+t) - r_i(t_{0j})\right)^2 \quad (3)$$

where N is the number of atoms in the system, n_t is the number of time origins, t is time, and t_{0j} is the initial timestep originating at time j [31, 32].

Unless noted, all diffusion simulations were run with FPMD in VASP at the equilibrium volume with the NVT ensemble and 216 atoms for 12 ps. Mean squared displacements were calculated after the first 200 time steps (0.4 ps) to avoid any initial equilibration period. The remaining time steps were divided into four equal blocks and the mean squared displacement was calculated as a function of time for each block. In this study, the number of time origins (n_t) is fixed to the half of the block size in order to avoid the noise that is otherwised observed at the last part of time steps. The use of half the block size for n_t ensures that each MSD values at the time of (t) are obtained from the same length of trajectory data. The diffusion coefficient is calculated for each

block by fitting the slope of the MSD vs. time. To obtain a robust linear region of the MSD data in the block, the first 25 time steps, which often show the expected quadratic MSD(t) dependence [31] are excluded. An error on D from a given block is then estimated from the fitting error in the slope of MSD vs. time following the statistical equations [33]. The final diffusion coefficient is the average of the diffusion coefficients of each block. The error of each diffusion coefficient from the linear fitting is propagated through the averaging over blocks to the final standard deviation of the mean. This block averaging method is similar to that of Rapaport [34].

3. Results

3.1. Creating converged liquid structures

Equilibrating a liquid molten salt from a solid, crystalline structure was not feasible within timescales of up to 18 ps at 1000K with FPMD (Fig. 1(a)). Radial distribution functions (RDFs) confirm that FPMD simulations starting from a solid structure still retain long-range order (Fig. 1(a)). While more disordered starting conditions and higher temperatures could certainly accelerate the convergence, we chose to simply initiate the FPMD results with IPMD data. IPMD simulations were used to equilibrate all liquid structures by the approach discussed in the Computational methods section and showed converged stable liquid RDFs (Fig. 1(b)) after equilibration following the approach described in the Computational methods section. The resulting equilibrated IPMD liquid was used as the starting structure for the FPMD calculations and stable liquid RDFs were obtained with FPMD (Fig. 1(c)). RDFs show the same liquid structure in IPMD and FPMD and longer simulations in the FPMD do not significantly alter the RDFs (although they do get smoother). The slight variations in Li-Li interactions between IPMD and FPMD are probably due to the differences between interatomic potentials and the full density functional theory of FPMD.

3.2. Testing convergence with simulation time

One concern of running FPMD for only 5-10 ps is that the time scales are not long enough to yield converged results for temperature, volumes, energies, pressures, and diffusivities. To test the convergence of these properties with simulation time, IPMD NVT simulations were started from the same converged IPMD simulation that would be used to start a VASP simulation (represented by t=0 in Fig. 2). Simulations with 64 atoms at 1096 K were run with IPMD for 6, 12, 20, 50, 100 and 200 ps (Fig. 2). We assess convergence by considering if the predicted value and errors at some smaller time are consistent with the value at the longest time, which we take to be essentially the exact prediction. This approach does not mean the shorter simulation has a small error bar, only that the values and errors are estimated robustly enough that they are consistent with the exact prediction.

Starting from an equilibrated liquid, a simulation time of 6 ps is long enough to obtain temperatures and energy values that are within the standard deviation of the mean of the values at 200 ps. The pressure at 6 ps is not within one standard deviation of the pressure at 200 ps; the pressure at 6 ps is slightly higher than the pressure at 200 ps by 0.07 ± 0.05 GPa. To obtain diffusion coefficients that are within a standard deviation of the diffusion coefficients at 50 ps, a simulation time of at least 12 ps is needed, especially for Cl (Fig. 2(d)). The standard deviation of the diffusion coefficient is still ~10% or more of its value of the self-diffusion coefficient, even after 50 ps.

3.3. Testing convergence with unit cell size

Additional convergence testing was run in IPMD to test if unit cells of ~50-200 atoms are large enough to give the same results as up to 1000-atom unit cells during the reasonable simulation time (100 ps) (Fig. 3). Simulations for 64, 100, 216, 400, and 1000 atoms were equilibrated in

IPMD using NVE (crude barostat), NPT (P=0) for 100,000 time steps, and the NVT for 100,000 time steps. Volumes and errors in Fig. 3(a) were obtained from NPT and pressure (b), energy (c) and temperature (d) were obtained from NVT simulations. Properties estimated using a unit cell size of 64 atoms and 100 atoms have larger error bars compared to the values at a bigger cell. Volume and pressure values estimated from a cell size of 64 atoms deviate ~1 % and 0.04 GPa, respectively, from the 1000-atom values. Estimated energies using a smaller cell also deviate ~5 meV/atom from the 1000-atom value. A unit cell of at least 216 atoms is needed for accurate energies. Temperature changes little with unit cell size however, the standard deviation decreases as the unit cell size increases. As can be seen in Fig. 3, a unit cell size of at least 216 atoms is preferable to obtain results that are converged with respect to larger unit cells. However, given a speed-up of an almost 8 times for a 64-atom unit cell over a 216-atom unit cell, 64-atom unit cells can be used for quicker testing without sacrificing significant accuracy.

3.4. Role of dispersion and exchange correlation

One approximation made within density functional theory is the treatment of the exchange correlation between electrons. Common choices include the local density approximation (LDA), which considers only the local electron density, and the Generalized Gradient Approximation with the PBE parameterization (PBE), which considers the gradient of the electron density. Additionally, the PBEsol [35] potential improves upon PBE for solids and is effective for alkali metals and alkali halides.

Differences amongst these exchange-correlation functions are often well known in solids, e.g., GGA typically overestimates volumes and LDA underestimates volumes [36]. These differences are not as well established in high-temperature molten salts. Multiple volumes were run for PBE, PBEsol and LDA in LiCl (64 atoms) and the resulting pressure-volume curves are shown in Fig. 4. Without dispersion, PBE yields the largest volume, the volume with PBEsol is ~ 5 % less than with PBE, and the volume with LDA is almost 30 % less than with PBE. The inclusion of dispersion corrections (see Computational methods section) lowers the pressure by up to 1 GPa. For PBE and PBEsol, adding dispersion decreases the volume by ~ 15-20 %. In the LiCl-KCl system, the best match to experimental volumes for all compositions is obtained with the PBE exchange correlations run with the inclusion of dispersion (DFT-D2 method). Therefore, unless noted, all future FPMD calculations in this work are done with PBE and DFT-D2 to include dispersion.

3.5. Equilibrium volumes, thermal expansion, bulk modulus

In order to determine equilibrium volume (V_0) from NVT simulations, multiple volumes were run for LiCl, KCl and the eutectic composition at multiple temperatures (Fig. 5). Experimental data are plotted as open markers for reference. The resulting pressure-volume data and resulting errors were fit to the Murnaghan equation of state to obtain V_0 and the equation of state properties (Table 1). In LiCl-KCl eutectic, the equilibrium volumes agree well with available experimental data for all temperatures, but equilibrium volumes are slightly underestimated or overestimated for LiCl and KCl (Fig. 5, Fig. 6, and Table 1).

Coefficients of thermal expansion [17, 37]:

$$\alpha_V = \frac{1}{V}\left(\frac{\partial V}{\partial T}\right)_P \tag{4}$$

at a specific volume were calculated for each composition and temperature from the slope of the volume vs. temperature plot (Fig. 6 and Table 2). Volumes as a function of temperature from FPMD are shown in comparison to experimental data (Fig. 6). Experimental data in the LiCl-KCl eutectic composition has the most variability. Calculated volumes for the eutectic composition fall within the error bars of the experimental data (dashed line). Volumes for LiCl are underestimated by about 4-5 % (~1 $Å^3$/atom) and volumes for KCl are overestimated by about 2-3 % (~1 $Å^3$/atom) by the calculations compared to the experiments.

Bulk modulus (*B*) decreases with increasing temperature (Fig. 7), consistent with Garai and Laugier [38]. LiCl has highest *B*; KCl has the lowest *B*. The eutectic *B* is between LiCl and KCl, as would be expected. The bulk modulus for these liquids is quite low (< 8 GPa) compared to solid LiCl (*B* ~30 GPa at room temperature) [39] and solid KCl (*B* ~17 GPa at room temperature) [38]. *B'*, the change in *B* with pressure, was difficult to constrain with values ranging from 4-12 and uncertainties of up to about ±2.

3.6. Diffusivity

The self-diffusion coefficients were calculated for Li, Cl and K in LiCl, KCl and LiCl-KCl with the eutectic composition (Fig. 8, Fig. 9 and Table 3). Experimental and IPMD computational data exists in the literature for comparison in both LiCl [9, 40-42] and KCl [9, 10, 19, 42, 43], but only IPMD computational data exists for self-diffusion in eutectic LiCl-KCl [9, 10].

Thre are a range of values in the experimental self-diffusion coefficients, with different experimental studies showing up to one order of magnitude difference (Morgan and Janz in Fig. 8(c) and (d)). For Li diffusivity in LiCl, the FPMD diffusion coefficients fall between the experimental diffusivity and IPMD (literature) results. Cl diffusivity in LiCl calculated from FPMD is slightly lower than the experimental values by Janz et al. [41] and previous IPMD calculations, and show a somewhat larger slope vs. temperature with temperature than data with the widest temperature range [40]. K and Cl diffusion in KCl from FPMD calculations are near experimental and previous IPMD results. The experimental data from Janz et al. [41] in KCl is significantly lower than any other study.

FPMD self-diffusion coefficients for Li, Cl and K in eutectic LiCl-KCl (Fig. 9) agree well with previous IPMD simulations [9, 10], although trends with temperature for Li are slightly steeper than the IPMD results. No error bars were reported in the IPMD simulations.

3.7. Gibbs Free Energy of Mixing

The Gibbs free energy of mixing (ΔG_{mix}) at a given temperature can be estimated from an ideal solution model as [37]:

$$\begin{aligned}\Delta G_{mix} &= E_{xLiCl-(1-x)KCl} - xE_{LiCl} - (1-x)E_{KCl} - TS_{mix} \\ &= E_{xLiCl-(1-x)KCl} - xE_{LiCl} - (1-x)E_{KCl} + RT\left[x\ln x + (1-x)\ln(1-x)\right]\end{aligned} \tag{5}$$

where x is the concentration of LiCl. Total energy values from FPMD with 64-atom unit cell (19 Li, 32 Cl, 13 K; x=0.594) were used to estimate the free energy of mixing at the eutectic composition at 1096 K. ΔG_{mix} from FPMD is in good agreement with the experimental fit (Fig. 10). The FPMD data is only lower than experimental fit by ~ 0.9 kJ/mol (< 10 meV/Cl atom), which is within our error tolerance for the FPMD simulations. This shows that the excess entropy of mixing for this molten salt system is close to zero at high temperature and the free energy of mixing can be estimated from the ideal solution model.

4. Discussion and conclusions

FPMD calculations were used to calculate the equilibrium volume at multiple temperatures, thermal expansion, bulk modulus, and self-diffusion coefficients for LiCl, KCl and eutectic LiCl-KCl molten salts as well as the Gibbs free energy of mixing. Convergence testing proved unit cells of 216 atoms and simulation times of 6-12 ps are sufficient for adequately converged results that overall agree well with experimental data and classical IPMD simulations. Convergence errors on FPMD data with these settings are small enough to provide useful information on salt properties while still being practical.

The results show that FPMD calculations are able to reliably calculate the equilibrium volume, using NVT simulations, with reasonable agreement with experiments (agreement to within 5 % for LiCl, agreement to within 3 % for KCl and 1 % LiCl-KCl). Statistical convergence errors on FPMD volumes are typically less than 0.1 $Å^3$/atom (less than 0.5 %). Previous simulations with IPMD and DFT-TB fixed the volume to experimental values [9, 10, 19, 20]. The Tosi-Fumi potentials used in IPMD simulations [9, 10] overestimate the experimental volume by 6-7 % (Fig. 4(a)) corresponding to a pressure of 0.31 GPa in the simulations [9]. The FPMD simulations, which calculate the equilibrium volume independent of experiments, can be extended to predict volumes and densities in systems where little or no experimental data exists.

Calculations can provide guidance when experimental measurements have a wide range of value, as in the self-diffusion coefficients shown in Fig. 8. Our FPMD results with 216-atoms have good agreement with most of the experimental measurements [9, 40-42] and the IPMD calculations [9, 10, 19, 42]. Although the results are not provided, even with just a 64-atom unit cell and simulations times of only 12 ps, FPMD can calculate diffusion coefficients with errors of less than 10 %.

FPMD simulations are a useful predictive tool for properties like bulk modulus, where no experimental data exists on the LiCl-KCl system. Even more complex thermodynamics, such as the Gibbs free energy of mixing, can be estimated with a simple ideal solution model, which makes aspects of phase stability accessible with FPMD.

With the exception of finding equilibrium volumes, the FPMD simulations shown here do not significantly improve upon IPMD simulations. Given the significant speedup of IPMD simulations relative to FPMD, IPMD simulations are most efficient for systems where quality potentials can be developed. The real benefit of FPMD simulations is for use in systems where accurate potential fitting proves problematic or there is interest in electronic properties, like redox chemistry or magnetic moment, that are difficult to simulate without full electronic structure methods. The validation shown in this work of FPMD simulations on LiCl-KCl system provides confidence in applying the same techniques to additional systems, including impurities in the LiCl-KCl system or entirely different salts.

This draft is published as: First-principles molecular dynamics modeling of the LiCl-KCl molten salt system, Amelia Bengtson, Hyo On Nam, Saumitra Saha, Ridwan Sakidja, Dane Morgan, Computational Materials Science, Volume 83, Pages 362–370, 2014

Acknowledgements

This research was performed using funding received from the DOE Office of Nuclear Energy's Nuclear Energy University Programs (NEUP 10-418). The authors acknowledge the Idaho National Laboratory's (INL) Center for Advance Modeling and Simulation (CAMS) for providing HPC resources that have contributed to the research results reported within this paper. This work also benefitted from the use of the Extreme Science and Engineering Discovery Environment (XSEDE), which is supported by National Science Foundation grant number OCI-1053575. About half the calculations were performed on each computer system. The authors thank Jacob Eapen, Brahmananda Chakraborty, and Jin Wang for many enlightening discussions on simulations in these molten salt systems. The authors also thank Christopher Woodward, who provided advice on running first-principles molecular dynamics simulations, including the addition of the kinetic energy term in VASP-MD.

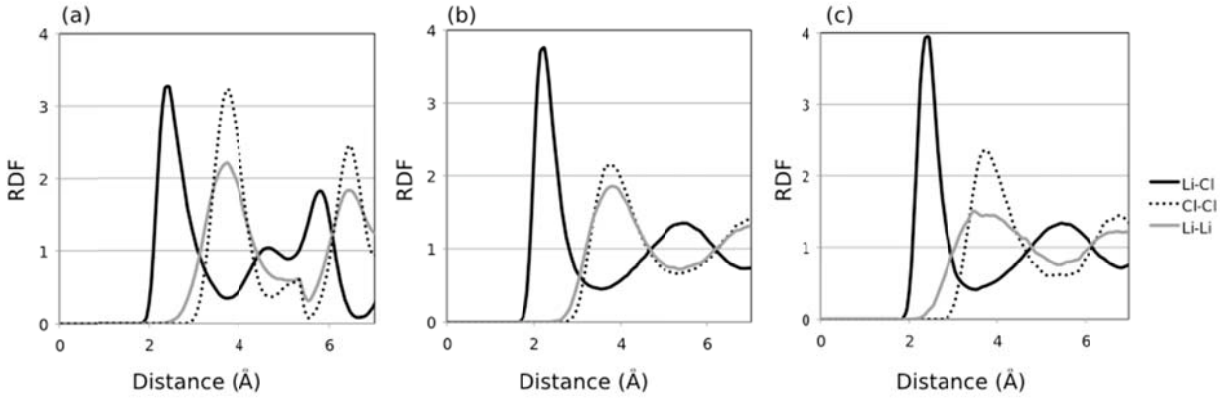

Fig. 1. Structural parameters for the 64-atom LiCl structure. (a) FPMD calculations started from solid, crystalline structure and run at 1000 K for 18 ps. Long-range order is not lost, suggesting the material is not molten. (b) Classical IPMD simulations using the LAMMPS code run for 100 ps. (c) FPMD calculations starting from liquid structure equilibrated in LAMMPS from part (b) run for 6 ps.

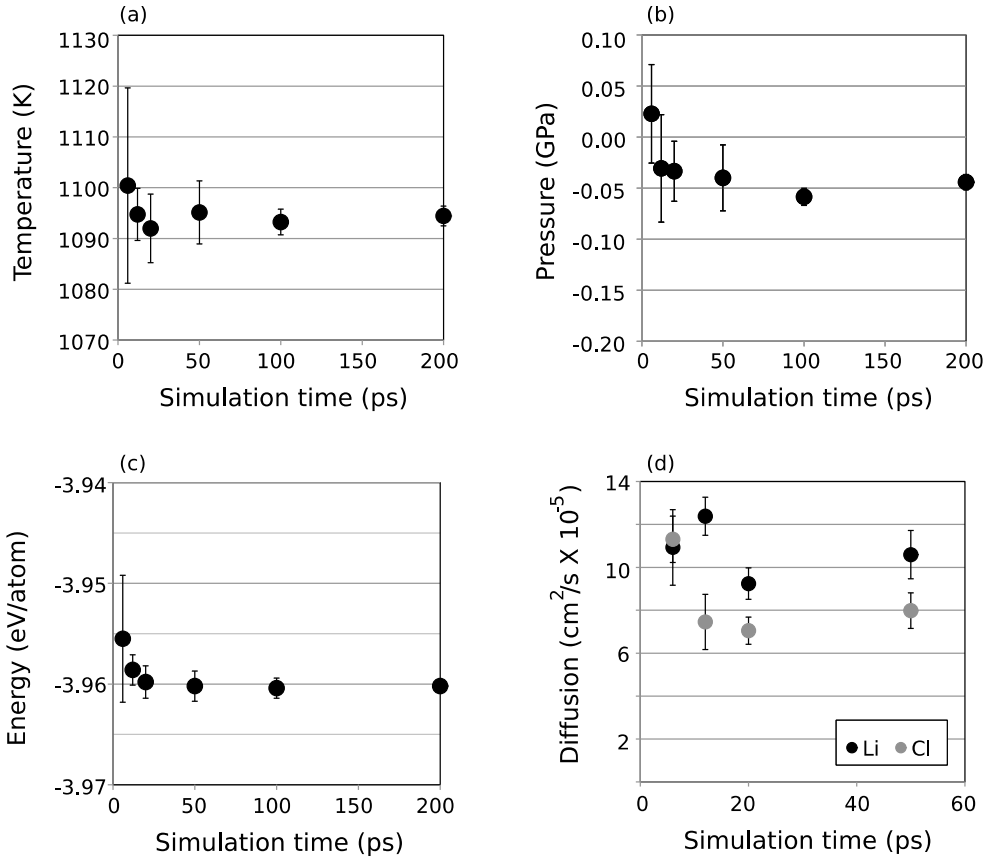

Fig. 2. Convergence of (a) temperature (b) pressure (c) total energy and (d) self-diffusion coefficients with simulation time. Simulations were run for 6, 12, 20, 50, 100, and 200 ps. All simulations were run as NVT with IPMD (using LAMMPS) for LiCl with 64 atoms at 1096 K with a timestep of 2 fs. All simulations started from the same converged IPMD simulation that would be used to start a VASP (FPMD) simulation. Desired simulation times for VASP are 5-10 ps. Errors were calculated from the autocovariance function. Averaging started after 0.5 ps so as to use only the equilibrated region.

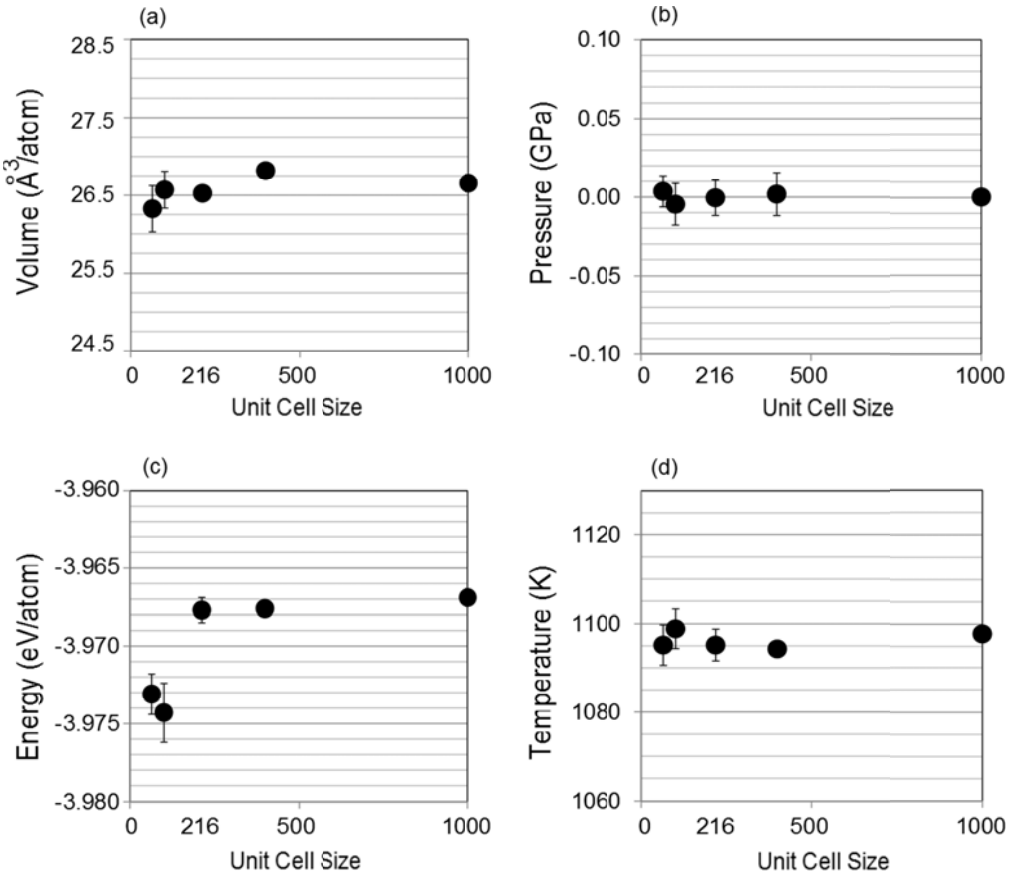

Fig. 3. Convergence of (a) volume (b) pressure (c) energy and (d) temperature with unit cell size in LiCl. Simulations were run with IPMD with the method outlined in the Computational methods section (NVE, crude barostat, NPT (P=0) for 100,000 steps, NVT for 100,000 steps). Volumes and errors in (a) come from NPT simulation analyzed over last 90% of data set. (b, c, d) results are from NVT simulations where the last 90% of simulation was analyzed. Errors are from analytical method.

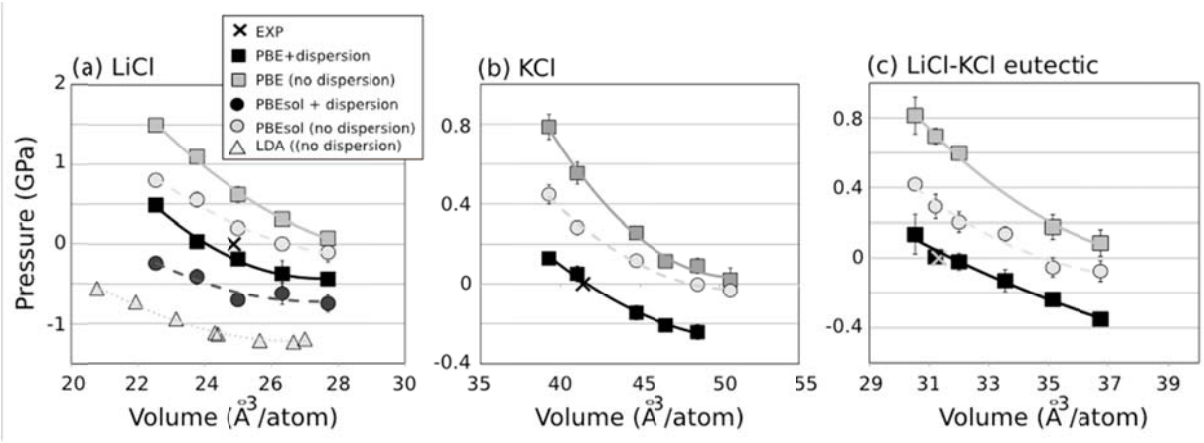

Fig. 4. Comparison of FPMD computational choices at 1096 K in VASP. All simulations were run with 64 atoms. PBE, PBEsol and LDA are different choices controlling the exchange correlation within a density functional theory calculation. EXP is experimental data from Janz et al. [41] either at 1096 K or extrapolated to 1096 K.

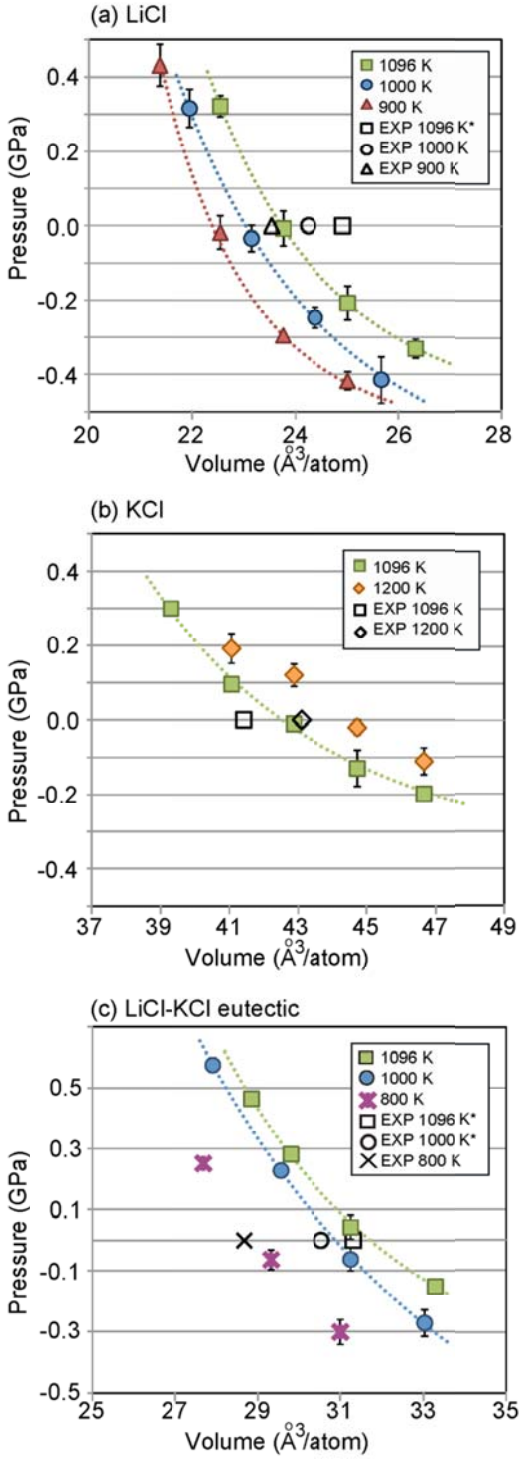

Fig. 5. Pressure-volume curves from VASP FPMD simulations with the NVT ensemble for of (a) LiCl (b) KCl and (c) LiCl-KCl with the eutectic composition. Experimental volumes are from (*extrapolated from) Janz et al. [41].

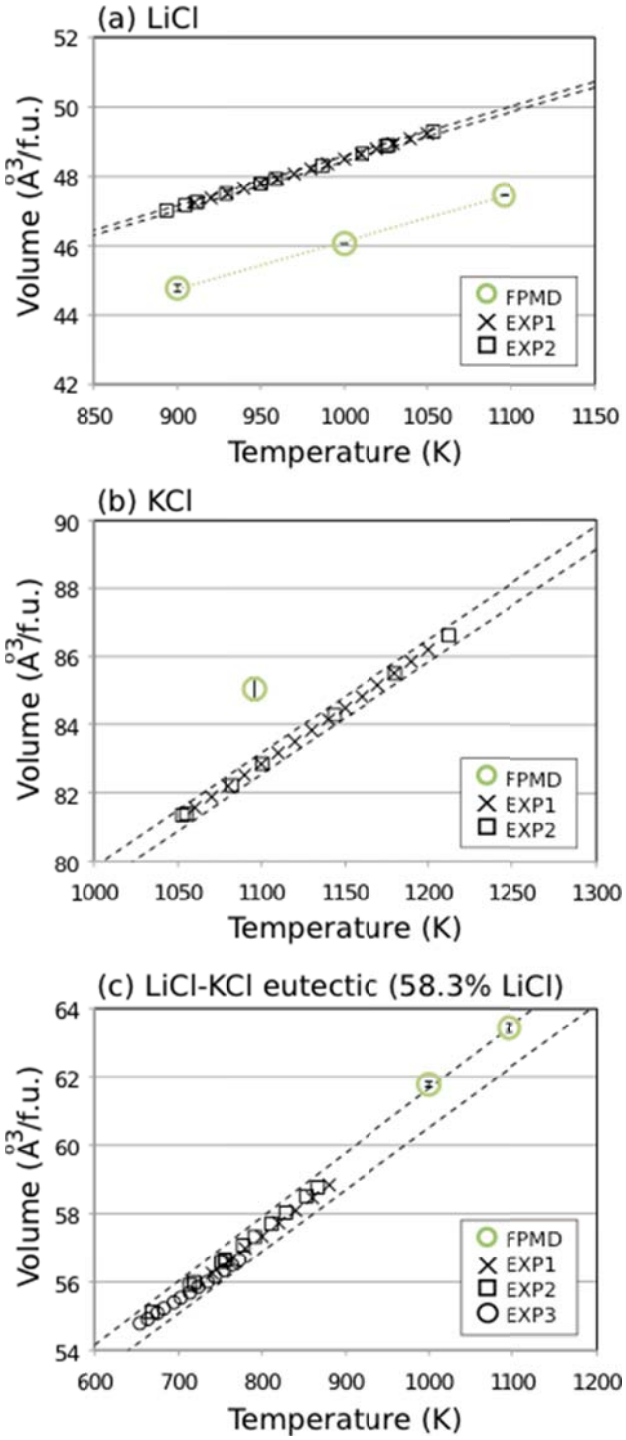

Fig. 6. Volume vs. temperature for (a) LiCl (b) KCl and (c) LiCl-KCl with the eutectic composition at multiple temperatures. LiCl-KCl volumes are plotted per Cl atom. EXP1 = Janz et al. (1979) [41]. EXP2 = Van Artsdalen and Yaffe (1955) [44], EXP3 = Ito et al. (2001) [45]. Dashed lines indicate the experimental error between the experimental datasets.

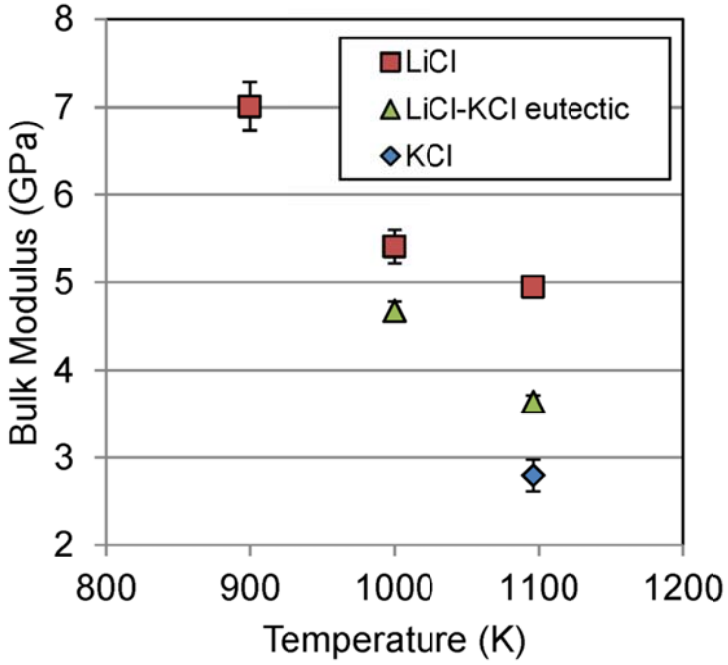

Fig. 7. Bulk modulus vs. temperature for the LiCl-KCl system.

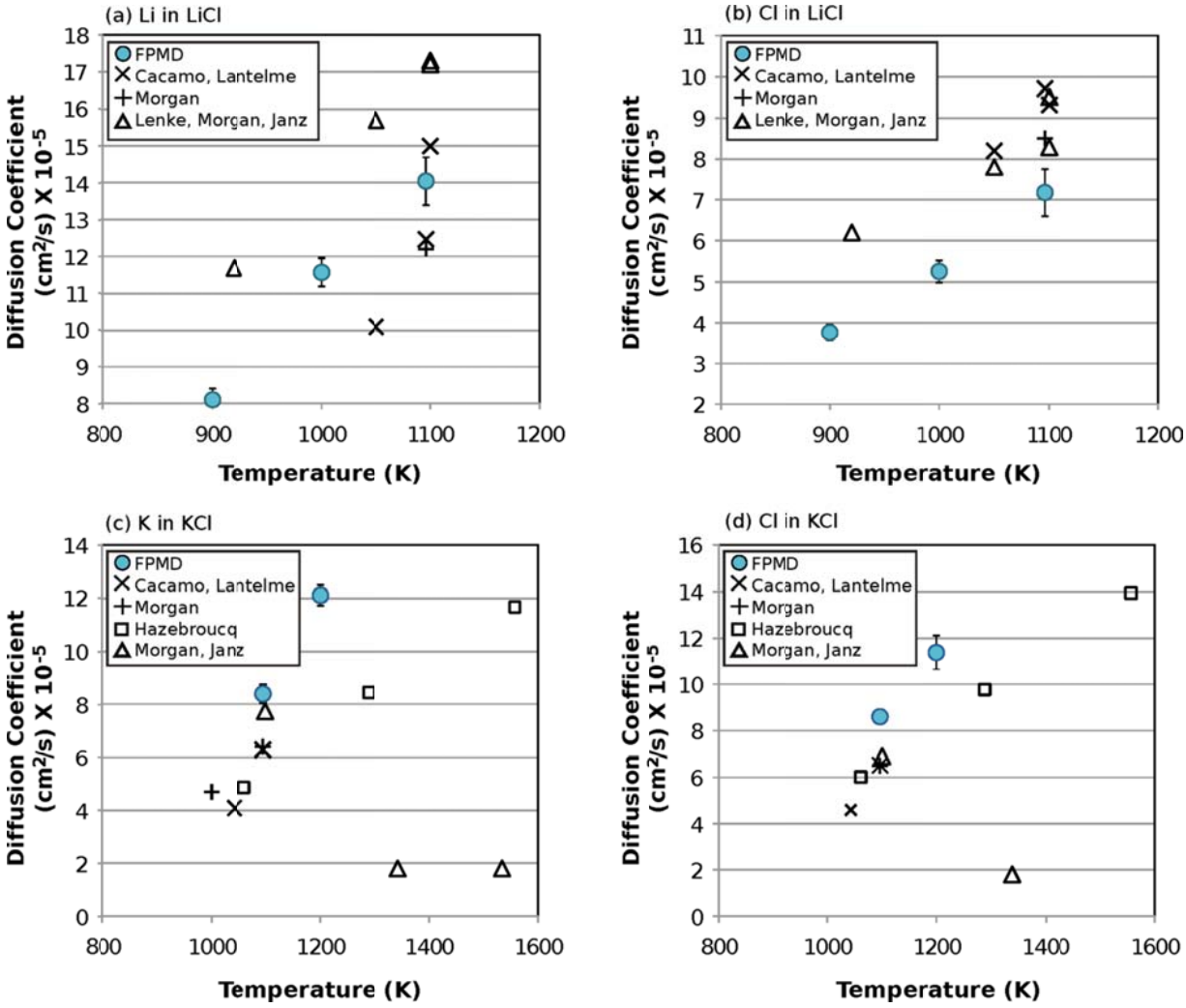

Fig. 8. Self-diffusion coefficients from FPMD simulations for (a) Li in LiCl (b) Cl in LiCl (c) K in KCl and (d) Cl in KCl. Experimental values for LiCl are from Lenke et al. [40] and Janz et al. [41] and references within Lantelme and Turq [9] and Morgan and Madden [42]. Computational IPMD values for LiCl are taken from Lantelme and Turq [9], Caccamo and Dixon [10], and Morgan and Madden [42] and references within. Experimental values for KCl are from Morgan and Madden [42] and Janz [43] and references within. Computational IPMD values for KCl are from Lantelme and Turq [9], Caccamo and Dixon [10], Hazebroucq et al. [19], and Morgan and Madden [42]. All simulations were run with FPMD in VASP at the volume closest to equilibrium (LiCl: 23.76 $Å^3$/atom at 1096K, 23.15 $Å^3$/atom at 1000K, 22.55 $Å^3$/atom at 900K; KCl: 44.74 $Å^3$/atom at 1200K, 42.88 $Å^3$/atom at 1096K) with the NVT ensemble and 216 atoms for 6 ps[1]. Analysis started after the first 200 time steps (for equilibration). The remaining time steps were divided into 4 equal blocks. The MSD vs. time curve was fit for all but the initial 25 steps of each block in order to avoid the quadratic region.

[1] Simulations in KCl were run for 5.4 ps (2689 time steps) at 1200K and 7.3 ps (3641 time steps) at 1096K.

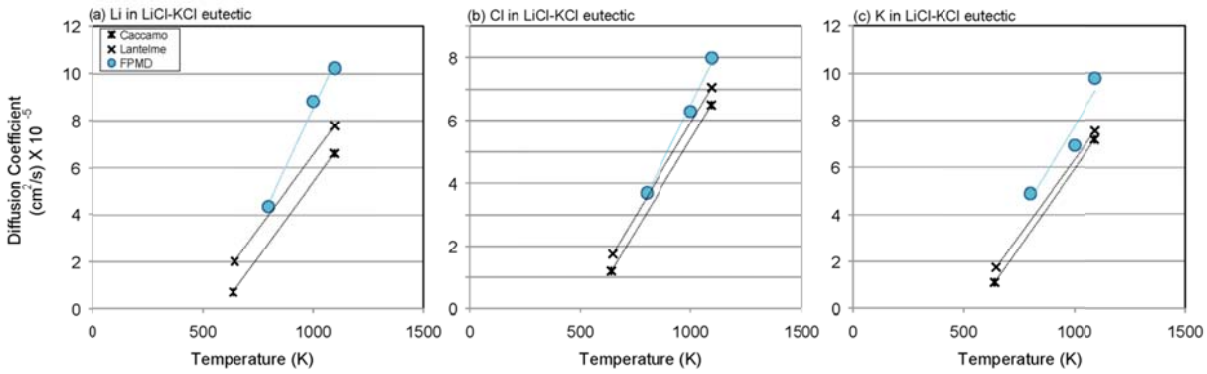

Fig. 9. Self-diffusion coefficients from FPMD simulations for (a) Li, (b) Cl and (c) K in eutectic LiCl-KCl. All simulations were run with FPMD in VASP at the volume closest to equilibrium (31.26 $Å^3$/atom at 1096K, 31.26 $Å^3$/atom at 1000K, and 29.31 $Å^3$/atom at 800K) with the NVT ensemble and 216 atoms for 6 ps[2]. Analysis started after the first 200 time steps (for equilibration). The remaining time steps were divided into 4 equal blocks. The MSD vs. time curve was fit for all but the initial 25 steps of each block in order to avoid the quadratic region. Results are plotted with IPMD simulations from the literature: Lantelme and Turq [9] and Caccamo and Dixon [10] .

[2] Simulations at 800K were only run for 5.5 ps (2744 time steps).

This draft is published as: First-principles molecular dynamics modeling of the LiCl-KCl molten salt system, Amelia Bengtson, Hyo On Nam, Saumitra Saha, Ridwan Sakidja, Dane Morgan, Computational Materials Science, Volume 83, Pages 362–370, 2014

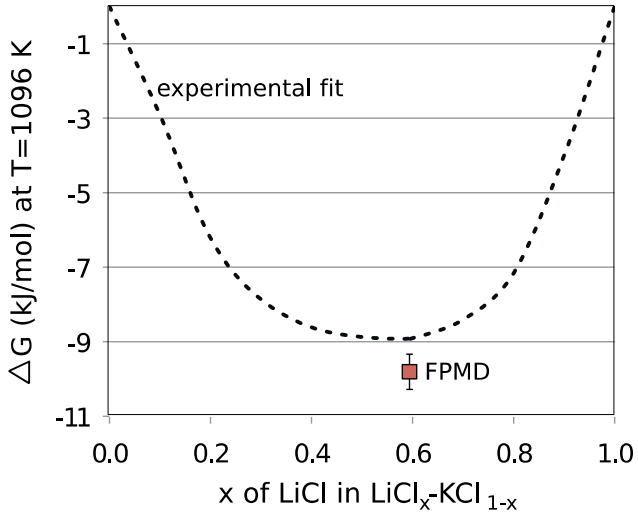

Fig. 10. Gibbs free energy at 1096 K. The fit to experimental data (dashed line) comes from the FTsalt - FACT salt database (FactSage). http://www.crct.polymtl.ca/fact/phase_diagram.php?file=KCl-LiCl.jpg&dir=FTsalt

Table 1
Equilibrium volume (V_0) from FPMD with 216 atoms. Simulations were run at multiple volumes for the NVT ensemble. V, P were fit to a Murnaghan equation of state to obtain V_0 (Experimental V_0: Janz et al. (1979) [41] (extrapolated for some temperatures))

	% LiCl	T (K)	V_0 Experiment (Å^3/atom)	V_0 (Å^3/atom)	B (GPa)	B'
LiCl	100	1096	24.93	23.73 ± 0.005	4.95 ± 0.02	9.30 ± 0.16
		1000	24.25	23.03 ± 0.001	5.41 ± 0.19	7.42 ± 1.35
		900	23.54	22.39 ± 0.052	7.01 ± 0.28	12.32 ± 1.70
KCl	0	1200	43.10	*Could not fit with EOS*		
		1096	41.42	42.52 ± 0.167	2.79 ± 0.18	6.90 ± 1.91
LiCl-KCl eutectic	58.3	1096	31.32	31.72 ± 0.064	3.64 ± 0.07	5.88 ± 0.90
		1000	30.54	30.89 ± 0.037	4.67 ± 0.11	3.69 ± 0.51
		800	28.67	*Could not fit with EOS*		

Table 2
Coefficient of thermal expansion, α_V at 1096 K from FPMD with 216 atoms.

	% LiCl	Temperature (K)	α_V FPMD (1/K) X 10^{-4}	α_V Experiment (1/K) X 10^{-4}
LiCl	100	1096	2.87	2.94 ± 0.00
KCl	0	1096	-	3.94 ± 0.02
LiCl-KCl	58.3	1096	2.73	2.93 ± 0.05

Table 3

Self-diffusion coefficients for Li, Cl and K in LiCl, KCl and eutectic LiCl-KCl. All simulations were run with FPMD in VASP at the volume closest to equilibrium with the NVT ensemble and 216 atoms for 6 ps[3]. Analysis started after the first 200 time steps (for equilibration). The remaining time steps were divided into 4 equal blocks. The MSD vs. time curve was fit for all but the initial 25 steps of each block in order to avoid the quadratic region.

	% LiCl	Volume Å^3/atom	Temp (K)	Diffusion Li cm^2/s x 10^{-5}	Diffusion K cm^2/s x 10^{-5}	Diffusion Cl cm^2/s x 10^{-5}
LiCl	100	23.76	1096	14.04 ± 0.66	-	7.18 ± 0.58
		23.15	1000	11.58 ± 0.39	-	5.26 ± 0.27
		22.55	900	8.10 ± 0.30	-	3.77 ± 0.20
KCl	0	44.74	1200	-	12.11 ± 0.39	11.38 ± 0.74
		42.88	1096	-	8.39 ± 0.36	8.6 ± 0.25
LiCl-KCl eutectic	59.4	31.26	1096	10.23 ± 0.84	9.78 ± 0.63	7.99 ± 0.68
		31.26	1000	8.83 ± 0.40	6.93 ± 0.24	6.29 ± 0.16
		29.31	800	4.37 ± 0.27	4.89 ± 0.50	3.70 ± 0.08

[3] Simulations in LiCl-KCl eutectic at 800 K were only run for 5.5 ps (2744 time steps). Simulations in KCl were run for 5.4 ps (2689 time steps) at 1200 K and 7.3 ps (3641 time steps) at 1096 K.

References

[1] J.L. Willit, W.E. Miller, J.E. Battles, Journal of Nuclear Materials, 195 (1992) 229-249.

[2] Y. Sakamura, T. Hijikata, K. Kinoshita, T. Inoue, T.S. Storvick, C.L. Krueger, L.F. Grantham, S.P. Fusselman, D.L. Grimmett, J.J. Roy, Journal of Nuclear Science and Technology, 35 (1998) 49-59.

[3] Y. Sakamura, T. Hijikata, K. Kinoshita, T. Inoue, T.S. Storvick, C.L. Krueger, J.J. Roy, D.L. Grimmett, S.P. Fusselman, R.L. Gay, Journal of Alloys and Compounds, 271 (1998) 592-596.

[4] S.X. Li, S.D. Herrmann, K.M. Goff, M.F. Simpson, R.W. Benedict, Nuclear Technology, 165 (2009) 190-199.

[5] D. Yamada, T. Murai, K. Moritani, T. Sasaki, I. Takagi, H. Moriyama, K. Kinoshita, H. Yamana, Journal of Alloys and Compounds, 444 (2007) 557-560.

[6] H.C. Eun, Y.Z. Cho, S.M. Son, T.K. Lee, H.C. Yang, I.T. Kim, H.S. Lee, Journal of Nuclear Materials, 420 (2012) 548-553.

[7] S. Vandarkuzhali, N. Gogoi, S. Ghosh, B.P. Reddy, K. Nagarajan, Electrochimica Acta, 59 (2012) 245-255.

[8] A. Aguado, P.A. Madden, Journal of Chemical Physics, 117 (2002) 7659-7668.

[9] F. Lantelme, P. Turq, Journal of Chemical Physics, 77 (1982) 3177-3187.

[10] C. Caccamo, M. Dixon, Journal of Physics C-Solid State Physics, 13 (1980) 1887-1900.

[11] M.C.C. Ribeiro, Journal of Physical Chemistry B, 107 (2003) 4392-4402.

[12] E. Mendes, R. Malmbeck, C. Nourry, P. Soucek, J.P. Glatz, Journal of Nuclear Materials, 420 (2012) 424-429.

[13] M. Salanne, C. Simon, P. Turq, P.A. Madden, Journal of Physical Chemistry B, 112 (2008) 1177-1183.

[14] V. Cristiglio, L. Hennet, G.J. Cuello, I. Pozdnyakova, M.R. Johnson, H.E. Fishcer, D. Zanghi, D.L. Price, Journal of Non-Crystalline Solids, 354 (2008) 5337-5339.

[15] N. Sun, L. Stixrude, N. de Koker, B.B. Karki, Geochimica Et Cosmochimica Acta, 75 (2011) 3792-3802.

[16] B.B. Karki, L.P. Stixrude, Science, 328 (2010) 740-742.

[17] C. Woodward, M. Asta, D.R. Trinkle, J. Lill, S. Angioletti-Uberti, Journal of Applied Physics, 107 (2010).

[18] S. Zahn, B. Kirchner, Journal of Physical Chemistry A, 112 (2008) 8430-8435.

[19] S. Hazebroucq, G.S. Picard, C. Adamo, T. Heine, S. Gemming, G. Seifert, Journal of Chemical Physics, 123 (2005).

[20] A. Klix, A. Suzuki, T. Terai, Fusion Engineering and Design, 81 (2006) 713-717.

[21] G. Kresse, J. Hafner, Physical Review B, 47 (1993) 558-561.

[22] L. Martínez, R. Andrade, E.G. Birgin, J.M. Martínez, Journal of Computational Chemistry, 30 (2009) 2157-2164.

[23] S. Plimpton, Journal of Computational Physics, 117 (1995) 1-19.

[24] H.J.C. Berendsen, J.P.M. Postma, W.F. Vangunsteren, A. Dinola, J.R. Haak, Journal of Chemical Physics, 81 (1984) 3684-3690.

[25] G. Kresse, J. Furthmüller, Computational Materials Science, 6 (1996) 15-50.

[26] G. Kresse, J. Furthmüller, Physical Review B, 54 (1996) 11169-11186.

[27] S. Nosé, Journal of Chemical Physics, 81 (1984) 511-519.

[28] S. Grimme, Journal of Computational Chemistry, 27 (2006) 1787-1799.

[29] C. Alexopoulos, in: Proceedings of the 38th conference on Winter simulation, Winter Simulation Conference, Monterey, California, 2006, pp. 168-178.

[30] F.D. Murnaghan, Proceedings of the National Academy of Sciences, 30 (1944) 244-247.

[31] M.P. Allen, D.J. Tildesley, Computer Simulation of Liquids, Clarendon Press, Oxford 1987.

[32] T. Croteau, G.N. Patey, Journal of Chemical Physics, 124 (2006).

[33] J.R. Taylor, An Introduction to Error Analysis: The Study of Uncertainties in Physical Measurements, University Science Books; 2nd edition (March 10, 1997), 1997.

[34] D.C. Rapaport, The Art of Molecular Dynamics, 2nd ed., 2004.

[35] J.P. Perdew, A. Ruzsinszky, G.I. Csonka, O.A. Vydrov, G.E. Scuseria, L.A. Constantin, X.L. Zhou, K. Burke, Physical Review Letters, 100 (2008).

[36] G.I. Csonka, J.P. Perdew, A. Ruzsinszky, P.H.T. Philipsen, S. Lebegue, J. Paier, O.A. Vydrov, J.G. Angyan, Physical Review B, 79 (2009).

[37] R.T. DeHoff, Thermodynamics in Materials Science, Second Edition, CRC Press, University of Florida, Gainesville, USA, 2006.

[38] J. Garai, A. Laugier, Journal of Applied Physics, 101 (2007) 023514-023514.

[39] U. Kohler, P.G. Johannsen, W.B. Holzapfel, Journal of Physics-Condensed Matter, 9 (1997) 5581-5592.

[40] R. Lenke, Uebelhac.W, A. Klemm, Zeitschrift Fur Naturforschung Section a-a Journal of Physical Sciences, 28 (1973) 881-884.

[41] G.J. Janz, C.B. Allen, R.M. Bansal, R.M. Murphy, R.P.T. Tomkins, in, National Bureau of Standards, U.S. Department of Commerce, 1979.

[42] B. Morgan, P.A. Madden, Journal of Chemical Physics, 120 (2004) 1402-1413.

[43] G.J. Janz, Molten Salts Handbook, Academic Press, 1967.

[44] E.R. Van Artsdalen, I.S. Yaffe, The Journal of Physical Chemistry, 59 (1955) 118-127.

[45] H. Ito, Y. Hasegawa, Y. Ito, Journal of Chemical and Engineering Data, 46 (2001) 1203-1205.